

Original Article

Generation, characterization, and maintenance of trastuzumab-resistant HER2+ breast cancer cell lines

Sandra Zazo^{1*}, Paula González-Alonso^{1*}, Ester Martín-Aparicio¹, Cristina Chamizo¹, Ion Cristóbal², Oriol Arp³, Ana Rovira³, Joan Albanell³, Pilar Eroles⁴, Ana Lluch⁴, Juan Madoz-Gúrpide^{1*}, Federico Rojo^{1*}

¹Department of Pathology, IIS-Fundación Jiménez Díaz, UAM, E-28040 Madrid, Spain; ²Translational Oncology Division, Onco Health Institute, Health Research Institute FJD-UAM, University Hospital Fundación Jiménez Díaz, Madrid, Spain; ³Department of Medical Oncology, Hospital del Mar, Barcelona, Spain; ⁴Institute of Health Research INCLIVA, Valencia, Spain. *Equal contributors.

Received September 16, 2016; Accepted September 19, 2016; Epub November 1, 2016; Published November 15, 2016

Abstract: Trastuzumab became the therapy of choice for patients with HER2-positive breast cancer in 1998, and it has provided clinical benefit ever since. However, a significant percentage of patients show primary resistance to trastuzumab at diagnosis, and most patients with metastatic disease that initially respond to trastuzumab eventually progress (acquired resistance). Consequently, there is an urgent need to improve our knowledge of the mechanisms governing resistance, so that specific therapeutic strategies can be developed to provide improved efficacy. We generated new cell lines derived from BCCL through extended exposure to trastuzumab. Drug-conditioned populations were authenticated for their molecular profile and their resistance rate was determined. Heterogeneous *HER2* amplification was observed across most of the BCCLs, ranging from cells without *HER2* amplification to elevated *HER2* gene copy numbers in others. Using a phospho-antibody array we analyzed the status of kinase receptors and effectors from different cellular pathways. This revealed that HER2, AKT, and S6RP presented high phosphorylation levels with specific variations between sensitive and resistant populations. In addition, differences in phosphorylation levels for several of those pathways targets were found between sensitive and resistant lines. Furthermore, a biochemical study characterized patterns of molecular alterations similar to those commonly described in breast cancer. Finally, a subcutaneous xenograft murine model confirmed the resistance to trastuzumab of the established cell line. We conclude that these resistant BCCLs can be a valuable tool to gain insight into the mechanisms of acquisition of trastuzumab resistance.

Keywords: Breast cancer, anti-receptor therapy, trastuzumab, cell lines, resistance

Introduction

Breast cancer is the leading cause of cancer-related death among women worldwide [1]. Breast cancer is a heterogeneous disease at the molecular level: about 20% of invasive breast cancers have high levels of HER2, either as a result of gene amplification or due to over-expression of the protein, both of which promotes the growth of the cancer cells [2]. For this reason, HER2+ subtypes are more aggressive than other types and also show poorer response to chemotherapy and hormonal treatments.

However, there are specific treatments targeting HER2 that are very effective. These include

trastuzumab, a monoclonal humanized murine antibody that binds to the extracellular domain of HER2 with high affinity [3, 4]. Trastuzumab improves the response rate, progression-free survival, and overall survival of patients with metastatic HER2-positive breast cancer [5]. Despite such effectiveness, its mechanism of action is not yet fully understood, and a significant percentage of patients present primary resistance to trastuzumab. In addition, many patients with metastatic disease that initially respond to trastuzumab progress after a period of exposure to the treatment (acquired resistance) [5].

For years, scientists worldwide have relied on cell lines to study how tumor cells respond to

different treatments. Such models are widely used in cancer research, since they are valuable for understanding the cellular and molecular biology of cancer. In cellular models, trastuzumab reduces the amount of HER2 molecules on the surface of the cell and produces anti-proliferative effects. In this study, we used trastuzumab as an *in vitro* inducer to establish four trastuzumab-resistant human breast cancer cell lines and verify their underlying biological characteristics.

Although the molecular and cellular effects of trastuzumab have been described extensively in *in vitro* and *in vivo* models, the mechanisms of action by which trastuzumab induces regression of HER2-overexpressing tumors are still not fully defined. Diminished receptor signaling may result from trastuzumab-mediated internalization and degradation of HER2 [6, 7]. Trastuzumab inhibits the formation of HER2 homodimers, which, despite being capable of producing transphosphorylation of the receptor, do not trigger the underlying signal cascade. This results in functional inactivation of the HER2 receptor, inhibits homodimer-mediated cell growth, and can partially prevent the formation of heterodimers [8]. When used *in vivo*, trastuzumab increases the apoptosis of tumor cells and has anti-angiogenic effects. On the other hand, it induces DNA breaks and repair defects [9], and it is also known to modulate the transcription of various genes involved in DNA repair mechanisms [10]. These data suggest that the effects of trastuzumab may be a causal factor behind the decreased cell proliferation and synergy seen between trastuzumab and many chemotherapeutic agents.

Potential mechanisms of resistance to trastuzumab have already been described in the literature, including: i) interaction of HER2 with other HER-family receptors (EGFR and HER3) [11]; ii) dimerization of HER2 with other types of receptors, such as IGF1R and c-MET [12, 13]; iii) increased expression of ligands from the EGF family [14]; iv) constitutive activation of signaling pathways such as PI3K/AKT, secondary to activating mutations of PI3K or inactivation of PTEN (loss, mutation, or methylation of the promoter) [15, 16]; v) amplification/overexpression of cyclin E [17]; vi) reduction in the expression of p27 [18]; and vii) presence of truncated forms of the receptor-p95. HER2-accommodating tyrosine-kinase activity [19].

Finally, mutations of EGFR and HER2 have also been described as factors of resistance to anti-receptor treatment [20]. Nevertheless, the prevalence of such mutations in the extracellular domain of HER2 is low.

We present a panel of cell lines derived from several models of HER2+ BCCLs with acquired resistance to trastuzumab caused by prolonged exposure to moderate doses of the drug. We confirmed the authenticity of these lines with a panel of specific mutations and histological analysis, studied the heterogeneity of the different cell populations through cytogenetic examination, and characterized the lines by immunohistochemistry (IHC), fluorescence in-situ hybridization (FISH), and biochemical analyses to verify the expression pattern of some targets of the routes associated with response and resistance to trastuzumab (PI3K/ATK and MAK). Finally, we established a nude mouse xenograft model, the results of which further substantiated the resistance of the trastuzumab-conditioned cell lines. The aim of this study was to develop different cellular models with acquired resistance to trastuzumab and validate their efficacy as tools to investigate the mechanisms of generation of such resistance.

Materials and methods

Cell lines, cell culture, and reagents

The effects of trastuzumab on cell growth were studied in a panel of ten HER2-amplified breast cancer cell lines, including a trastuzumab-conditioned HER2-amplified cell line selected for long-term out growth in a trastuzumab-containing medium. The cell lines AU-565 (CRL-2351) adenocarcinoma, BT-474 (HTB-20) ductal carcinoma, HCC1419 (CRL-2326) ductal carcinoma, HCC1569 (CRL-2330) metaplastic carcinoma, HCC1954 (CRL-2338) ductal carcinoma, MDA-MB-361 (HTB-27) adenocarcinoma, SK-BR-3 (HTB-30) adenocarcinoma, and UACC-812 (CRL-1897) ductal carcinoma were obtained from the American Type Culture Collection. The EFM-192A (ACC-258) metastasizing breast adenocarcinoma and JIMT-1 (ACC-589) ductal carcinoma cells were obtained from the German Tissue Repository DSMZ. All cell lines were checked for authentication every 6 months, either by using the Cell Line Authentication service at LGC Standards (UK) (tracking no: 710259498; 710274855; 710281607; 71027-

Trastuzumab-resistant HER2+ breast cancer cell lines

Table 1. Panel of primers selected for the characterization of the breast cancer cell lines

A. Primers designed for <i>Mycoplasma</i> detection						
	Target gene	FW primer	RV primer	UPL probe	Amplicon length	
	16S ribosomal RNA [<i>Mycoplasma</i> sp.]	5' GAGCAAACAGGATTAGATACCC 3'	5' GATGATTTGACGTCATCCCC 3'	#69	416 bp	
	RPP30	5' CAGATGTTGGGTACTAATGAC 3'	5' CCAGGTATCTTCAGTAAAGTG 3'	#26	88 bp	
B. Primers for specific point mutations distinctive of different BCCL						
cell line	target gene	mutation	wt primer (5'-3')	mutation primer (5'-3')	common primer (5'-3')	location
BT-474	NFKB2	p.D865N [GAC>AAC] qPCR conditions:	FW: 5' CCCCAGCAGAGGTGAAGGAAG 3'	FW: 5' CCCCAGCAGAGGTGAAGGAAA 3'	RV: 5' GCAGGCAGCAGGTGAGTG 3'	NC_000010.1
SK-BR-3	TP53	p.R175H [CGC>CAC] qPCR conditions:	FW: 5' ATGACGGAGGTTGTGAGGCG 3'	FW: 5' ATGACGGAGGTTGTGAGGCA 3'	RV: 5' CAACCAGCCCTGTCGTCTCT 3'	NC_000017.10
AU-565		id.	id.	id.	id.	id.
	SMAD4	p.D355N [GAC>AAC] qPCR conditions:	FW: 5' GTTACTGTTGATGGATACGTGG 3'	FW: 5' GTTACTGTTGATGGATACGTGA 3'	RV: 5' CTCAATGGCTTCTGTCTGTG 3'	NC_000018.9
EFM-192A	NOTCH2	p.D661E [GAT>GAA] qPCR conditions:	FW: 5' GTATCCATGGAATCTGTATGGAT 3'	FW: 5' GTATCCATGGAATCTGTATGGAA3'	RV: 5' GAGCAGACACAACCTGTAGCGAT 3'	NC_00001.10
MDA-MB-453	PTEN	p.E307K [GAG>AAG] qPCR conditions:	RV: 5' CCTTGTCAATTATCTGCACGCTC 3'	RV: 5' CCTTGTCAATTATCTGCACGCTT 3'	FW: 5' TCTTCATACCAGGACCAGAGG 3'	NC_000010.10

Trastuzumab-resistant HER2+ breast cancer cell lines

2355) or by running a home-made mutational profiling assay. BT-474, SK-BR-3, MDA-MB-361, UACC-812, and JIMT-1 cells were maintained in DMEM-F12 supplemented with 10% heat-inactivated fetal bovine serum (FBS), 2 mmol/L glutamine, and 1% penicillin G-streptomycin. AU-565, HCC1419, HCC1569, and HCC1954 cells were cultured in RPMI 1640 supplemented with 10% heat-inactivated FBS, 2 mmol/L glutamine, and 1% PSF. EFM-192A cells were grown in RPMI 1640 medium supplemented with 20% heat-inactivated FBS, 2 mmol/L glutamine, and 1% PSF. Cells were maintained at 37°C with 5% CO₂.

Detection and cleaning of mycoplasma contamination by qPCR

Cell culture infection with bacteria of the genus *Mycoplasma spp.* can cause alterations in the phenotypic characteristics of the cell line and resistance to the drug [21]. To avoid this, cells in culture were routinely assessed for *Mycoplasma* contamination using two different PCR methods: i) the Universal Mycoplasma Detection kit (ATCC catalog number 30-1012K) was employed for initial and final verifications, as well as routinely every 1 year, according to manufacturer instructions; and ii) a home-made assay was used for routine checking every 2 months. Briefly, gDNA samples were extracted from cell cultures with the High Pure PCR Template Preparation kit (Roche, Switzerland). Primers were designed using the DNASTar Primer Design software (DNASTar Inc., USA) and the NCBI database. Our *Mycoplasma* assay combined specific primers for *Mycoplasma* with primers for the sequencing of human RNaseP (*RPP30* gene). *RPP30* was used as a reference gene to control DNA extraction and the performance of the qPCR. It is a single copy gene per haploid genome that is unamplified and located on chromosome 10 (10q23.31) (COSMIC dataset). The primers were designed to amplify the conserved 16S ribosomal RNA coding region within the *Mycoplasma* genome. Our design was specific for 11 different *Mycoplasma* species, and it did not recognize human gDNA (**Table 1A**). The assay combined the primers with a qPCR probe from the Universal Probe Library System Technology (Roche). Trials were conducted in triplicate, under laminar flow, and in the dark. To prepare the Master Mix, 1 × LightCycler 480

UPL buffer, 0.2 μM FW and RV primers, and 0.1 μM of the corresponding UPL probe were added, vortexed, and processed in the LightCycler 480 II real-time PCR System (Roche), in accordance with the MIQE guidelines [22]. Specific qPCR conditions were: an initial cycle of denaturation for 10 min at 95°C, followed by 45 cycles in two steps (one of 10 s at 95°C, and another 30 s at 60°C), and finally an unlimited cycle of cooling at 4°C. The results obtained and crossing point (Cp) values were processed in the LightCycler 480 software (Roche). Cp values showed a standard deviation of < 0.25. Cells with a positive result for the detection of *Mycoplasma* were treated with the elimination reagent Plasmocin (InvivoGen, USA): 25 μg/ml of Plasmocin was diluted in the appropriate culture medium. The treatment lasted for two weeks [23].

Establishment of four trastuzumab-resistant breast cancer cell lines (acquired resistance)

The trastuzumab-conditioned BT-474.R cell lines were established by culturing the BT-474 cell line in the appropriate medium supplemented with 15 μg/ml of recombinant humanized monoclonal HER2 antibody, trastuzumab (Herceptin, Genentech, USA). Trastuzumab was dissolved in sterile water at a stock concentration of 20 mg/ml. Resistant populations were obtained for the four cell lines through lifetime exposure to the drug for a minimum of 3 months in the case of the line SK-BR-3, 7 months in the case of the AU-565 and EFM-192A lines, and 8 months in the case of the BT-474 line. The concentration and precise method of resistance generation were selected based on previous reports in the literature [17, 24]. Cells were grown at 10 μg/ml trastuzumab in culture medium for 30 days, at which point the dose was increased to a final concentration of 15 μg/ml. Simultaneously, the parental lines were grown without treatment to maintain their sensitivity to the drug intact so that they could be employed as procedural controls. Once the establishment of resistance was confirmed, the cells were kept at a 15 μg/ml maintenance dose.

Determination of the resistance rate

Establishment of drug resistance was confirmed by cell proliferation assay, as determined in P100 plates containing 3-5 × 10⁶ cells

Trastuzumab-resistant HER2+ breast cancer cell lines

for each condition (sensitive and resistant), both grown in the absence and in the presence of trastuzumab for 7 days. The results were processed using the algorithm described by O'Brien, which correlates the rate of growth between the treated and non-treated cells, reflecting the doubling time of the cells [25]. Once the resistance was confirmed, cells were maintained in the absence of treatment for 30 days. After this pause period, resistance was reconfirmed using the same protocol [26]. Resistance was also confirmed after cycles of freezing and thawing. Resistant cell-line populations were maintained with 15 µg/ml of trastuzumab in the medium for months. Periodically, vials of both the sensitive (parental) and resistant cell populations (pools and clones) were stored in liquid nitrogen to keep a stock of young cells.

Cell growth assays

Cells were seeded in triplicate in p100 plates at a density of 500,000 cells per plate and allowed to adhere and enter growth phase before being treated with or without 15 µg/ml trastuzumab for 7 days in the appropriate culture medium. Cells were then harvested by trypsinization and counted using the TC20 Automated Cell Counter (BioRad, USA). The appropriate culture media and trastuzumab were replaced every 3 days.

Cell proliferation assay

Cells were seeded at a density of 10,000 cells per well in a 96-well plate and incubated overnight in appropriate complete medium. Cells were treated with 0.01-500 µg/ml trastuzumab. After 72 h of incubation, cell viability was determined using the MTS tetrazolium substrate assay (CellTiter 96 Aqueous One Solution Cell Proliferation Assay, Promega, USA) following the manufacturer's instructions. The absorbance was measured at 490 nm using a spectrophotometer. All experiments were repeated three times, with readings taken at least in triplicate for each concentration.

Clonogenic assay

Sensitive and resistant BT-474 cells were seeded in P100 plates in duplicate (2,000 cells per plate), and 24 h later they were treated with either 1 µg/ml trastuzumab or vehicle. Both the

medium and the treatments were changed every 3 days. After 21 days' treatment, colonies were stained with crystal violet dye, and the number and area were estimated using the ImageJ program (NIH).

Establishment of resistant xenografts and mouse studies

All animal work was conducted as per the Barcelona Biomedical Research Park (PRBB) Institutional Animal Care and Scientific Committee guidelines. Briefly, five-week-old female severe combined immunodeficiency (SCID/beige) mice (Charles River, USA) were implanted with 0.72 mg, 60-day release, 17 h estradiol pellets (SE-121 Innovative Research of America). The next day, 2.5×10^5 cells suspended in 1:1 PBS growth factor-reduced Matrigel (200 µL) were injected subcutaneously in the right flank via a 22-gauge, 1.5-inch needle. For therapeutic studies, BT-474 and BT-474.R cell lines were injected following the same protocol. Once tumors reached a volume of 100 mm³, the mice were randomly allocated to treatment consisting of trastuzumab 10 mg/kg or IgGκ 10 mg/diluted in sterile PBS and administered via intraperitoneal injection twice a week. Tumor diameters were serially measured with digital calipers and tumor volumes were calculated according to the formula: volume = width² × length/2. At the end of the experiment, tumors were harvested and formalin-fixed.

Protein extraction and quantification

Cells were washed with 3 ml PBS at RT. Next, cells were scraped in the presence of 150 µl lysis buffer (RIPA, proteinase inhibitor, phosphatase inhibitor) at 4°C and transferred to a 1.5-ml tube. Cells were incubated in lysis buffer for 20 min at 4°C and sonicated afterwards. Then the cell lysate was spun at 13,000 × g for 10 min at 4°C and the supernatant was retained and stored. Protein extracts were quantified using the Pierce BCA protein assay kit (Thermo Fisher Scientific, USA), following the manufacturer's instructions.

Western blotting (WB)

Protein aliquots were prepared at 1 µg/µl in 4 × Laemmli loading buffer and boiled at 95°C for 6 min. Twenty nanoliters of protein extract were

Trastuzumab-resistant HER2+ breast cancer cell lines

loaded in a 10% polyacrylamide gel (SDS-PAGE). Then, proteins were transferred to a nitrocellulose membrane for 1 h at 100 V and 4°C. The membrane was blocked (5% milk in PBST 1 ×) for 1 h, washed 3 × 10 min, and incubated with the primary antibody at RT overnight under agitation. The antibody concentrations used were as follows: HER2 (1:500); pHER2-Tyr1221/1222 (1:1000); AKT (1:1000); pAKT-Thr308 (1:1000); pAKT-Ser473 (1:1000); p44/42 MAPK (Erk1/2)-Thr202/Tyr204 (1:1000); S6 ribosomal protein (S6RP) (1:1000); pS6RP-Ser235/236 (1:1000) (Cell Signaling, USA); and GAPDH (1:5000) (Sigma Aldrich, USA). All primary antibodies were rabbit monoclonal antibodies. Next the membranes were washed for 3 × 10 min in PBST and incubated with a secondary antibody (diluted in 2.5% BSA in PBS 1 ×) at RT for 1 h. ECL-anti-mouse and ECL-anti-rabbit secondary antibodies attached to peroxidase (HRP; GE Healthcare, USA) were used at a concentration of 1:5000. The membranes were washed again 3 × 10 min and plunged into the detection reagent (ECL or ECL Prime, if applicable; Amersham, GE Healthcare) for 1 min, prior to developing on photographic film. Densitometry and quantification of proteins were carried out using ImageJ software.

Nucleic acid preparation

DNA or RNA were extracted from cellular pellets using either the High Pure PCR Template Preparation kit (Roche) or the RNeasy Mini kit (QIAGEN), following the manufacturers' instructions. The extracts were quantified in a NanoDrop 2000 spectrophotometer (Thermo Fisher Scientific) at 260 nm and subsequently stored at -20°C (DNA) or -80°C (RNA).

Authentication profiling of BCCL by mutational analysis

The analysis of the mutational profile is required to confirm the identity of the BCCLs under study. According to the panel of mutations described in the Cancer Cell Line Encyclopedia (CCLE) (<http://www.broadinstitute.org/ccle>), specific point mutations were chosen for different genes in the different cell lines, so that every cell line was unequivocally identified by a specific mutation. Mutations are not modified by the process of resistance generation, which allows the tracking of the resistant cell line back to the parental line. Additionally, *TP53* was selected because although its sequence contains point mutations in all cell lines includ-

ed in the study, the modified nucleotides are not the same. This makes *TP53* useful for the discrimination of SK-BR-3 and AU-565, which otherwise share the mutation p.R175H (**Table 1B**).

The assays were conducted in triplicate, under laminar flow, and in the dark. Three primers were designed for each gene: a wild-type (wt) primer, a point mutation primer (mut), and a common primer. Primers were designed so that the 3' end of either the FW or the RV primer would match the mutated nucleotide position. All primers were designed using the DNASTar software and the NCBI database. To establish the mutational profile of every BCCL, two different PCRs were prepared for each gene: one for the wt profile and one for the mutated profile. PCRs were carried out from 2 µl of gDNA (5 ng/µl) in a 384-well plate. To prepare the Master Mix, 1 × ResoLight buffer, 2 µM Mg²⁺, 0.2 µM FW, and RV primers were added, vortexed, and processed in the LightCycler 480 II real-time PCR System (Roche). Specific qPCR conditions consisted of an initial denaturation cycle for 10 min at 95°C, followed by 45 cycles in two/three steps (one of 10 s at 95°C, a second of 30 s at 60-64°C, and a conditional step of 20 s at 72°C), and finally an unlimited cycle of cooling at 4°C. The results obtained and the crossing point (Cp) values were processed in the LightCycler 480 software (Roche) and calculated based on the second derivative method.

Molecular characterization of trastuzumab-resistant cell lines

The same methods and criteria as those defined for the clinical diagnosis of tumor samples in patients with cancer of the breast (hormonal estrogen (ER) and progesterone receptors (PR) expression levels, as well as expression of the HER2 receptor, determined by IHC and FISH) were used for the molecular characterization of the BCCLs [27]. To this end, cell pellets were generated from 0.5-1 × 10⁷ cells, included in FFPE blocks, and cut in 2-3-µm slices. In parallel, we visually assessed morphological changes in resistant populations. As a result, images of cells in culture were captured on a regular basis.

Immunohistochemistry (IHC)

Immunostaining was performed using 3-µm FFPE sections of breast cancer cellular pellets, placed on plus-charged glass slides on a Dako

Trastuzumab-resistant HER2+ breast cancer cell lines

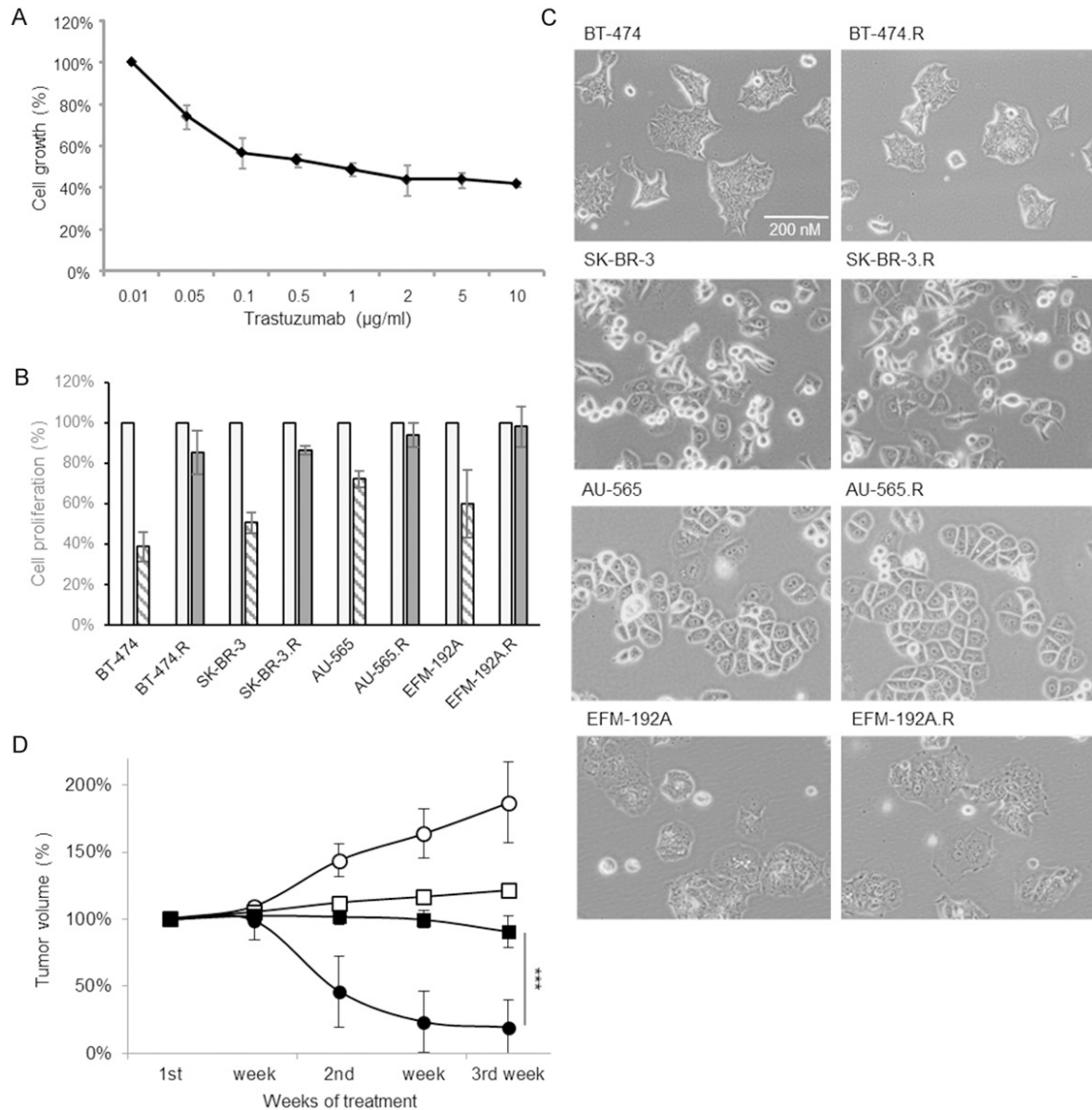


Figure 1. A. The effect of trastuzumab on the viability of the BT-474 (parental, sensitive) cell line for 72 h remains constant as of 10 µg/ml. The horizontal axis shows the different concentrations of trastuzumab (0.01 to 10 µg/ml, nonlinear scale) used to test the line BT-474. The values of cell growth are represented on the vertical axis and show that IC50 remains constant at concentrations greater than 10 µg/ml. B. Generation of acquired resistance to trastuzumab in cell lines BT-474, SK-BR-3, AU-565, and EFM-192A. Monthly cell count (average of a minimum of 3 replica) to assess the generation of resistance in the cell lines after sustained exposure to trastuzumab (10 µg/ml, first month; 30 days' pause; 15 µg/ml, later). In all cases resistant cells (dark gray boxes) showed a higher growth rate in the presence of the drug than the sensitive cells (pattern fill). Every trastuzumab-treated condition was compared to its corresponding non-treated one (light gray bars). C. Phase contrast images showing cultured monolayers of parental and trastuzumab-resistant cells for every BCCL. Morphological characteristics did not differ between sensitive and resistant cells of the same line. D. BT-474.R cells were resistant to trastuzumab *in vivo*. Female SCID/beige mice were injected with BT-474 (round markers) or BT-474.R cells (square markers) into the subcutaneous space. Once tumor volumes reached approximately 100 mm³, five mice per group were randomized to either IgGk 10 mg/kg (open markers) or trastuzumab 10 mg/kg (filled markers). Overall, significantly higher growth rates of BT-474.R cells were detected between initial and final days of treatment with trastuzumab, as compared to BT-474 cells ($P < 0.001$). Points: mean tumor volume of five mice per group; bars: SD.

Link platform (Dako, Agilent Technologies, USA). After deparaffinization, heat antigen

retrieval was performed in a pH 9 EDTA-based buffered solution (Dako). Endogenous peroxi-

Trastuzumab-resistant HER2+ breast cancer cell lines

dase was quenched. Primary antibodies were incubated for 30 min at RT: anti-estrogen receptor α (clone EP1) rabbit monoclonal antibody (IS084 Dako) ready to use, anti-progesterone receptor (clone PgR636) mouse monoclonal antibody (IS068 Dako) ready to use, and HercepTest (K5207 Dako). Antigen-antibody reaction was detected by incubation with an anti-mouse/rabbit Ig-dextran polymer coupled with peroxidase (Flex+, Dako). Sections were then visualized with 3,3'-diaminobenzidine and counterstained with hematoxylin. All immunohistochemical staining was performed on a Dako Autostainer platform.

Fluorescent in situ hybridization (FISH) for HER2/neu

FISH was performed according to the PathVysion (Vysis Inc., USA) guidelines, which appear in the package insert and are approved by the U.S. Food and Drug Administration. In brief, the PathVysion guidelines involve the rehydration of a paraffin-embedded 5- μ m-thick section. The section was air-dried, pretreated, and digested with proteinase K before being hybridized with fluorescent-labeled probes for the HER2 gene, and a-satellite DNA for chromosome 17. Nuclei were routinely counterstained with an intercalating fluorescent counterstain, DAPI. For each tumor, 60 tumor cell nuclei from invasive areas were identified using a Nikon Eclipse E400 fluorescence microscope with a rhodamine and FITC double filter, and scored for both HER2 and chromosome 17 centromere numbers. HER2 gene amplification was defined as a HER2-to-chromosome 17 ratio of ≥ 2.0 , as required by the guidelines.

Anti-phospho-tyrosine kinase antibody array assay

We employed the PathScan® RTK Signaling Antibody Array Kit (Chemiluminescent Readout) #7982 (Cell Signaling) to identify and relatively quantify the abundance level of phosphorylated forms of 28 receptors and 11 effectors from different cellular pathways (RTK, phospho-Receptor tyrosine kinase). Cell extracts were harvested in the lysis buffer included in the commercial kit, quantified for protein content with a BCA assay (Pierce), incubated in the array, hybridized against the printed antibody spots, and finally their signals were detected with a chemiluminescent substrate, following the manufacturer's protocol. Images were

obtained after automatic processing with an Amersham Imager 600RGB (GE Healthcare), and then underwent densitometric analysis using the software ImageQuant TL v8.1. After a negative control signal was subtracted from every spot, specific target intensity signals were normalized with respect to the positive control. Fold-change values were calculated for every target in every cell line. Median and range values were observed for every cell line.

Statistical analysis

For *in vivo* experiments, data was expressed as the mean \pm SE. The statistical significance of the differences between means were determined using a Student's t-test for two samples after verifying that data passed the normality test and the groups compared had equal variance. Differences were statistically significant at $P < 0.05$.

Results and discussion

Assessment of sensitivity to trastuzumab in HER2-positive breast cancer cell lines

The IC₅₀ values for trastuzumab were determined in the cell lines by studying cell viability using MTS proliferation assay. Based on reports appearing in the literature, the trastuzumab concentration range selected was 0.01-500 μ g/ml. The antiproliferative effects of trastuzumab were observed from drug concentrations as low as 0.5 μ g/ml, with a stabilizing level at around 10 μ g/ml (**Figure 1A**). Based on these findings and on existing reports, a working trastuzumab concentration of 15 μ g/ml was selected as suitable for the generation of cellular resistance.

Sensitivity to trastuzumab was assessed in a panel of 8 breast cancer cell lines by testing cell proliferation in the presence and absence of 15 μ g/ml trastuzumab for 7 days (**Supplementary Figure 1**). Both the medium and the drug were replenished every 3 days. Response to trastuzumab was quantified by calculating the change in the growth rate of the treated versus the non-treated cells, according to the algorithm described by O'Brien [25]. Therefore, cell lines with a growth rate fold increase of ≥ 1.2 were considered resistant in response to trastuzumab. Using this cutoff, the BT-474, SK-BR-3, AU-565, and EFM-192A cell lines were considered sensitive to trastuzumab.

Trastuzumab-resistant HER2+ breast cancer cell lines

Table 2. A panel of 12 parental and derived BCCLs were tested for trastuzumab response. Cells were classified as sensitive (S) or resistant (R) by testing cell proliferation in the presence and absence of 15 $\mu\text{g/ml}$ trastuzumab for 7 days. Response to trastuzumab was quantified by calculating the fold change in the growth rate (ΔGR) of the treated cells relative to the non-treated cells. In all cases resistance was defined as a response of ≤ 1.2 in growth rate

Cell line	Trastuzumab (15 $\mu\text{g/ml}$)			Response
	Cell viability	SD	Growth rate (fold change) (ΔGR)	
HCC1419	83.97%	0.08	1.15	R
HCC1596	117.52%	0.09	0.82	R
HCC1954	101.14%	0.02	0.94	R
JIMT-1	82.60%	0.08	1.11	R
BT-474	38.70%	0.07	3.52	S
BT-474.R	85.31%	0.11	1.14	R
SK-BR-3	50.67%	0.05	2.13	S
SK-BR-3.R	86.25%	0.02	1.11	R
AU-565	72.15%	0.04	1.26	S
AU-565.R	93.96%	0.06	0.91	R
EFM-192A	60.00%	0.17	1.73	S
EFM-192A.R	98.00%	0.10	0.85	R

ab, while the lines HCC1419, HCC1569, HCC1954, and JIMT-1 were considered resistant to treatment with trastuzumab (**Table 2**).

Generation of breast cancer cell lines resistant to trastuzumab (acquired resistance)

Three trastuzumab-resistant populations were generated from each sensitive cell line. After analyzing the effect of different concentrations of trastuzumab (**Figure 1A**) and as described in the literature, resistance was induced through continuous exposure to the drug over a variable period of time, ranging from 3-8 months. Cells were treated with 10 $\mu\text{g/ml}$ trastuzumab for the first 30 days, subsequently increasing the concentration to 15 $\mu\text{g/ml}$. Every corresponding parental cell line was simultaneously grown in parallel without treatment. This ensures the maintenance of their sensitivity to the drug, while providing a procedural control for every cell line. Progression of resistance was evaluated monthly by testing the cell proliferation in the presence and absence of trastuzumab at 7 days. Once the generation of resistance was confirmed, the treatment was paused for 30 days. For every cell line, between two and four pools were generated, and for each cell line we selected those with the highest percentage of

growth after 7 days of trastuzumab exposure (**Figure 1B**). After the monthly pause, cell counts confirmed acquired resistance to trastuzumab in the different BCCLs with respect to their corresponding sensitive controls. The clonogenic assay showed that BT-474. R cells improved their proliferation rates with respect to the parental BT-474 line after 21 days of trastuzumab treatment, close to the competence of the primary-resistance HCC1569 cell line: the number of colonies increased from 60 to 80% in the presence of 1 $\mu\text{g/ml}$ trastuzumab with respect to the untreated cells; the average colony area increased in the resistant population with respect to the sensitive one, and that area was almost the same size under treatment conditions (while the sensitive BT-474 cells decreased their average area size to a third); finally, the percentage of colony area after treatment rose from 20 to 60% in the BT-474.R line (**Supplementary Figure 2**). On the other hand, the morphological characteristics of the cells remained identical between the parental and the equivalent resistant cell lines (**Figure 1C**).

Generation of breast cancer mouse xenografts resistant to trastuzumab

We next transferred these results to an *in vivo* model by injecting BT-474 and BT-474.R cells into SCID/beige mice. Similar to *in vitro* culturing conditions, resistant cells exhibited slightly lower growth rates when injected into mice. All mice formed tumors measuring $\sim 100 \text{ mm}^3$. Treatment of established BT-474 xenografts with 10 $\mu\text{g/mg}$ trastuzumab for 3 weeks prevented the tumor growth from 100% to 19% with respect to day 0-cells, whereas administration of trastuzumab to BT-474.R xenografts prevented tumor growth from 100% to 91% (**Figure 1D**). These data suggest that resistance to trastuzumab is a stable phenotype in our generated BT-474.R cells.

Detection of contamination by *Mycoplasma*

qPCR assays designed to detect the presence of *Mycoplasma* contaminants in cell lines in culture showed differences in the amplification curves generated for each population (**Supplementary Figure 3**). Cp values lower than 30, which are indicative of gene amplification, confirmed the presence of *Mycoplasma* (**Supplementary Table 1**). Initially, BT-474 paren-

Trastuzumab-resistant HER2+ breast cancer cell lines

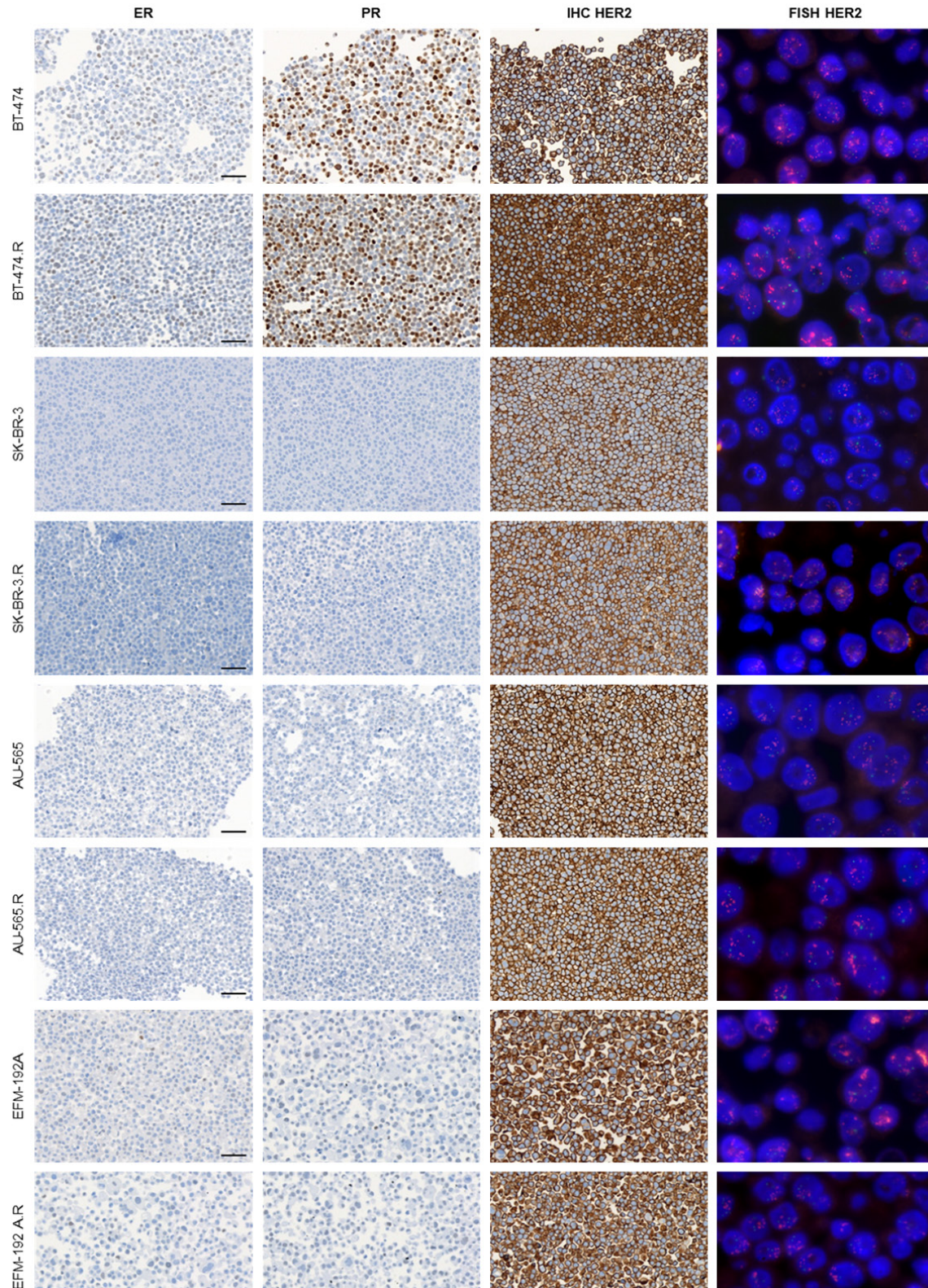


Figure 2. Characterization of the BCCLs by IHC profile and FISH. IHC detection of ER, PR, and HER2 expression in FFPE breast cancer cell lines. Sensitive and resistant populations of each cell line did not show changes in their molecular profile. The BT-474 cell line was confirmed as triple positive (ER+, PR+, and HER2+) and presents HER2 gene amplification (ratio HER2/CEP17 signals > 5). AU-565 and SK-BR-3 lines are HER2+, hormonal receptors negative (ER-, PR-), and have HER2 gene amplification (ratio > 6). The line shows 25 μ m. Magnification: x400. Abbreviations: ER, estrogen receptor; PR, progesterone receptor; S, sensitive; R, resistant; T, trastuzumab.

Trastuzumab-resistant HER2+ breast cancer cell lines

Table 3. Amplification signal of the *HER2* gene as determined by FISH. BCCL that showed ratio > 2.0 and > 4 HER2 copies were labeled as amplified, and those cases with ratio < 2.0 and 4-6 HER2 copies were determined as equivocal. Heterogeneity was observed as the percentage of tumor cells with ratio < 2.0 and < 4 HER2 copies

Cell line	Number of HER2 copies	Number of CEP17 copies	Ratio HER2/ CEP17	% tumor cells with ratio < 2.0 and < 4 HER2 copies
HCC1419	34.67	3.92	9.38	0.00%
HCC1569	12.17	2.22	7.62	20.73%
HCC1954	27.26	3.42	7.65	12.38%
JIMT-1	12.76	1.81	7.88	2.35%
BT-474	35.40	1.72	22.40	0.00%
BT-474.R	30.17	1.88	17.77	0.00%
SK-BR-3	8.04	4.93	1.64	14.39%
SK-BR-3.R	10.35	3.59	3.18	12.28%
AU-565	17.55	3.18	6.00	0.00%
AU-565.R	16.17	2.67	6.62	0.00%
EFM19-2A	14.62	1.95	9.07	15.08%
EFM19-2A.R	13.57	2.32	6.49	16.01%

tal cells showed positive signs of contamination by *Mycoplasma* (signal cycle 25.84), whereas the resistant pool (BT-474.R) exhibited the highest Cp value, indicating no presence of *Mycoplasma*. The Cp values of the AU-565 line (sensitive and resistant AU-565.R) were high, so no contamination was considered in those cell populations. SK-BR-3 (sensitive and resistant SK-BR-3.R) showed very low Cp values, thus confirming the presence of *Mycoplasma* in the culture. Similarly, EFM-192A cells also displayed low Cp values. Therefore, the initial analysis of *Mycoplasma* contamination by qPCR testing confirmed the presence of contamination in some cell lines under study. Afterwards, all the cell lines were treated with the cleaning compound Plasmocin and were subsequently reassessed for the presence of *Mycoplasma* contamination. The results showed an absence of curve amplification, indicating that the cleaning had been successful and confirming the elimination of any trace of contamination by *Mycoplasma*.

Molecular mutational profiling of trastuzumab-resistant cell lines

The qPCR tests designed for the detection of point mutations showed different patterns of amplification curves depending on the precise BCCL (Supplementary Figure 4). The presence of a gene mutation in a cell line was confirmed when the difference in Cp values between the

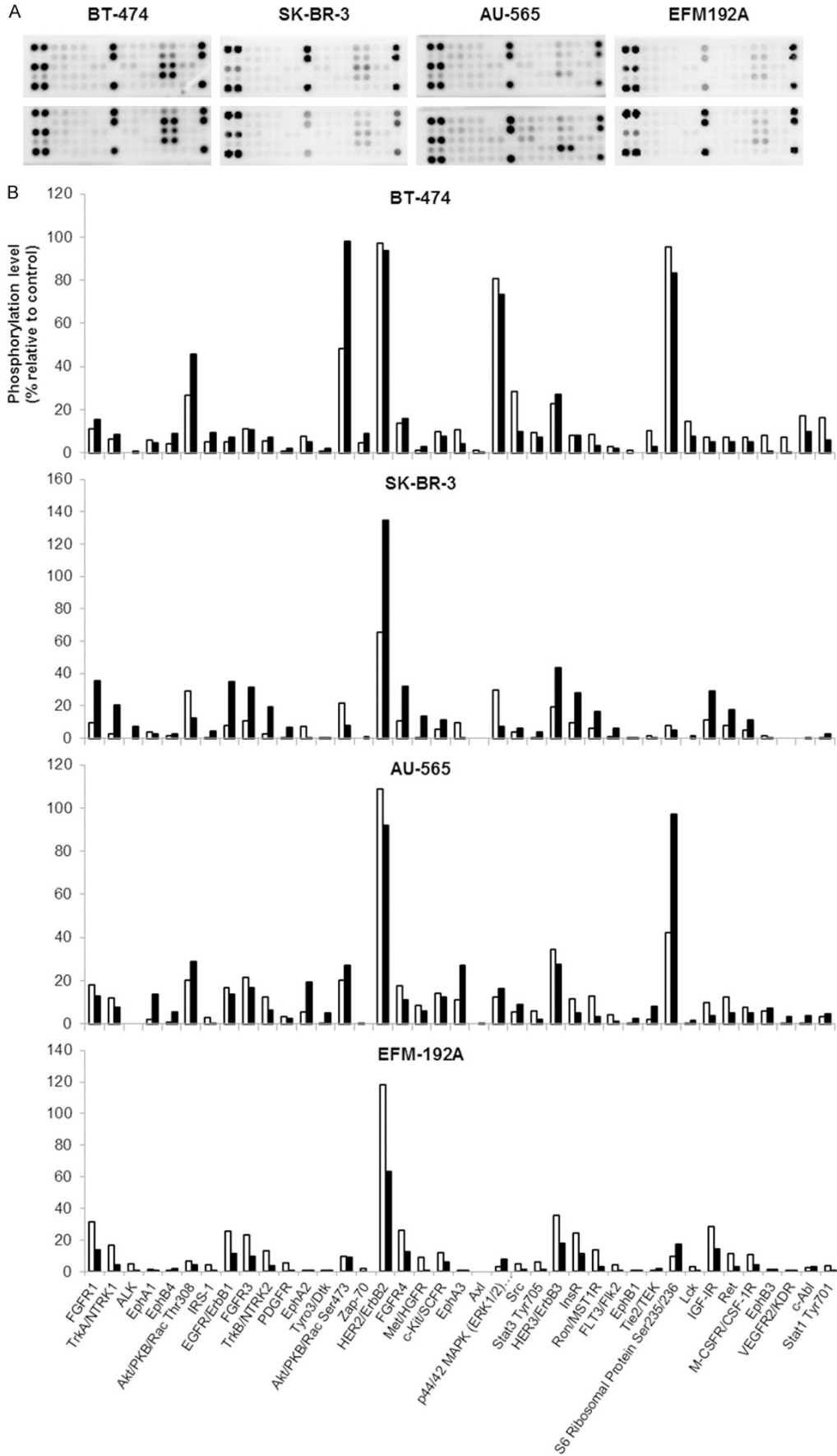
parental and the resistant cells showed a lower value than in the rest of the lines (functioning as a negative procedural control) (Supplementary Table 2). BT-474 (sensitive and resistant) cells have the lowest difference in Cp value for the *NFkB2* gene (wt and mutant assays). Differences in Cp values between trials for wt and mutant *TP53* in AU-565 cells (sensitive and resistant) and SK-BR-3 (sensitive and resistant) were much lower than values in

other lines. At the same time, AU-565 cells also showed an inferior value for the *SMAD4* mutation test. Finally, the line EFM-192A showed the lowest difference in Cp values between wt and mutant trials for the *NOTCH2* mutation assay. Therefore, analysis of the mutational profile by qPCR specific assays confirmed the identity of every BCCL included in the study.

IHC and FISH analyses helped to characterize the molecular profiles of the cell lines, and to assign every BCCL to their corresponding molecular subtype (Figure 2). Consequently, IHC identified the presence or absence of ER, PR, and HER2 overexpression and assigned positive or negative signals to the lines according to the receptor staining intensity. Positive nuclear staining for ER and PR was detected in the lines BT-474, BT-474.R, EFM-192A, and EFM-192A.R. No nuclear staining was detected for either of these receptors in the SK-BR-3, SK-BR-3.R, AU-565, or AU-565.R cell lines. Overexpression of HER2 (3+) was detected by IHC in all the lines. According to these criteria, the study lines were categorized in the following way: BT-474 and EFM-192A were ER+, PR+, and HER2+ (triple positive); and AU-565 and SK-BR-3 were luminal/HER2+ (ER- and PR-, and HER2+).

The existence of amplification was determined by FISH analyses (60 cell nuclei per sample), depending on HER2/CEP17 (red/green signal

Trastuzumab-resistant HER2+ breast cancer cell lines



Trastuzumab-resistant HER2+ breast cancer cell lines

Figure 3. A. Acquired resistance to trastuzumab alters the phosphorylation pattern of a panel of 39 specific tyrosine kinases in the BT-474, SK-BR-3, AU-565, and EFM-192A cell lines. Around 1.5×10^6 cells were grown per plate (except for BT-474, 1.7×10^6 cells). Data were compared for sensitive and resistant cell types. A. Image obtained after chemiluminescent revealing the hybridization reaction between cell line extracts and specific anti-tyrosine antibodies printed in a nitrocellulose-covered, glass slide array. The image was scanned in an Amersham Imager 600RGB detector and analyzed with the ImageQuant TL v8.1 software. B. Relative quantification of phosphorylation intensity signals for the different targets, with respect to the positive control. In addition to the elevated baseline intensity of pHER2 in every BCCL, signaling nodes (pAKT-Thr308, pAKT-Ser473, pERK1/2, and pS6RP) showed the most significant increase. Open white bars: sensitive cell lines; black bars: resistant cell lines.

signals) ratio. The samples that showed a ratio ≥ 2 were taken as HER2-amplified. Amplification of the *HER2* gene was detected in all the BCCLs under study (**Table 3**). Consequently, all BCCLs were characterized as amplified for HER2 signaling (BT-474, AU-565, and EFM-192A, with a ratio of HER2/CEP17 > 2 , and SK-BR-3 with a ratio < 2 and a HER2 copy number ≥ 6). Two hundred cores were evaluated in each line, according to the ASCP/CAP 2013 criteria [28]. Amplification of HER2 was confirmed in all cases with HER2/CEP17 ratio ≥ 2 and average HER2 copy number ≥ 4.0 signals/cell. The number of HER2 signals detected in the cell lines with acquired resistance was very similar to the signals detected in their corresponding parental cell line. Heterogeneity in the *HER2* amplification profile was observed in most of the lines, with a variable percentage of cells (1-20%) without *HER2* amplification (HER2/CEP17 ratio < 2 and number of copies of HER2 < 4), and a wide range of *HER2* copy number in all the BCCLs (**Supplementary Figure 5**). This finding was common to both sensitive (SK-BR-3, EFM-192A) and primary-resistant cell lines (HCC-1569, HCC1954, JIMT-1). In acquired-resistant cell lines we identified a percentage of cells with a ratio < 2 and HER2 copy number < 4 (SK-BR-3.R, 12% and EFM-192A.R, 16% respectively) and that was very similar to their corresponding parental lines (SK-BR-3, 14%; EFM-192A, 15%) (**Supplementary Figure 6**). Tumor heterogeneity-genetic, phenotypic, and functional-has been demonstrated in recent decades, both at the inter- and intra-cellular level [29, 30]. And clonal evolution was proposed in 1976 to explain how successive rounds of clonal selection give rise to tumors with diverse molecular alterations [31]. The variation that we found in the whole range of BCCLs under study is illustrative of the heterogeneity of tumor cell populations.

Importantly, all these data confirmed that matched sensitive and resistant populations

did not show changes in their molecular profiles of the markers. Firstly, the molecular characterization confirmed the identity of the cell lines, avoiding risks of potential cross-contaminations during the cell-culturing phase of resistance generation. Secondly, it ruled out that acquisition of secondary resistance to trastuzumab-based therapy would proceed through substantial changes at the HER2 receptor expression level. Although contradictory reports appear in the literature [32-35], we confirmed that trastuzumab did not down-regulate HER2 receptors in acquired-resistant BCCLs after months of treatment (**Figure 2** and **Table 3**). Instead, it is known that several other molecular mechanisms could contribute to the development of trastuzumab resistance [36]: increased signaling via alternative pathways (mainly phosphatidylinositol 3-kinase/AKT) could contribute to trastuzumab resistance because of activation of multiple receptor pathways that include HER2-related receptors [11, 37] or non-HER receptors (insulin-like growth factor 1 receptor) [12].

Phosphorylation status of protein membrane-receptor and signaling nodes

We used an antibody array as a screening tool to simultaneously detect the relative phosphorylation changes of 49 different RTKs in the cell lines with acquired trastuzumab-resistance, in comparison to their parental lines (BT-474, BT-474.R, SK-BR-3, SK-BR-3.R, AU-565, AU-565.R, EFM-192A, and EFM-192A.R). The signal showed a high specificity for the phosphorylated targets, with low background noise for each of the 8 cell lines under study (**Figure 3A**). As expected, the signal for HER2 was phosphorylated in all cases. At the same time, the quantification analysis showed that few targets exhibited elevated phosphorylation levels (around 50% of positive control signal). Most of the targets presented low phosphorylation signals, with only about 10% of the analyzed tar-

Trastuzumab-resistant HER2+ breast cancer cell lines

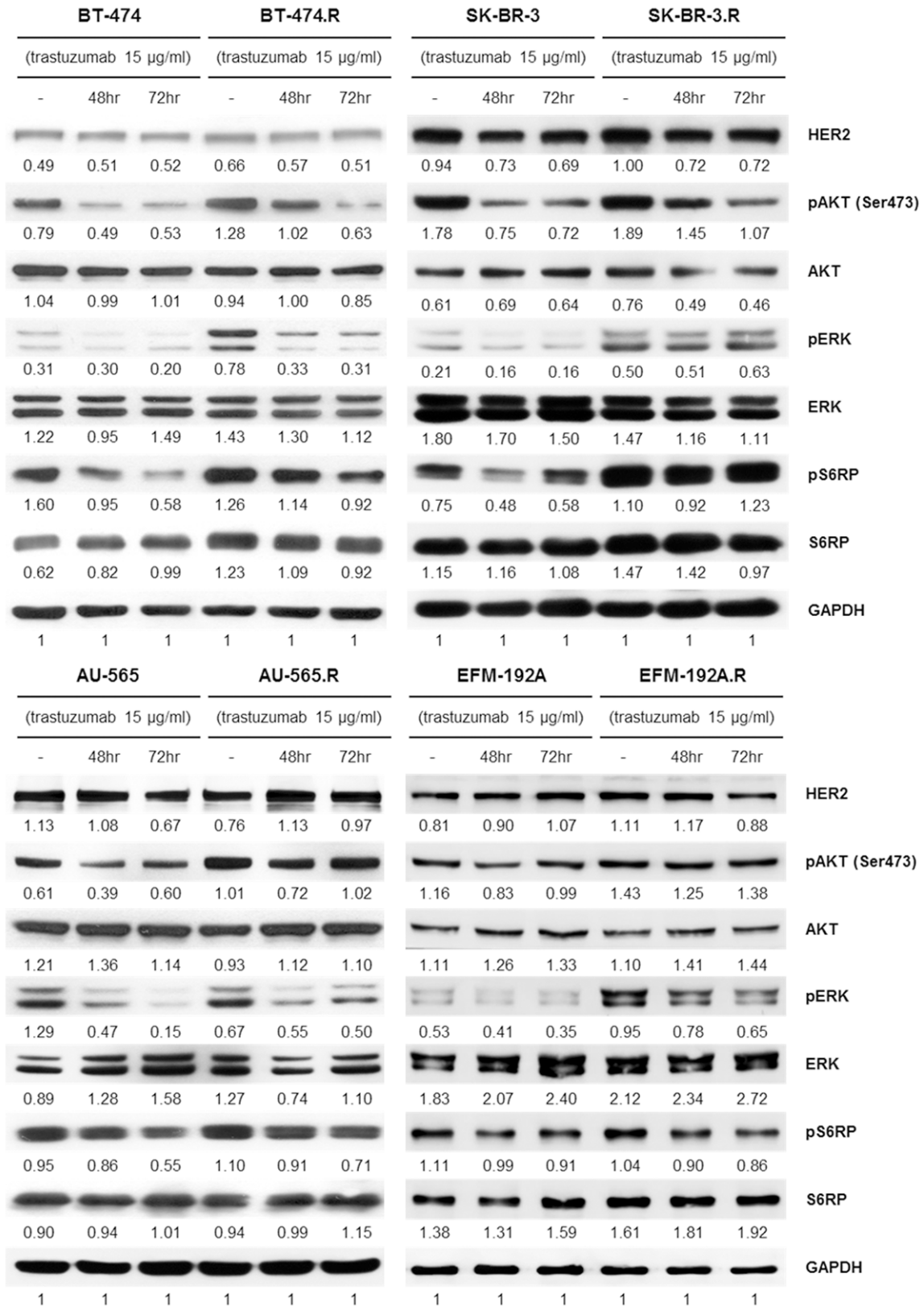


Figure 4. The generation of trastuzumab resistance induced changes in markers phosphorylation patterns in BC-CLs. Trastuzumab-sensitive and -resistant BT-474, SK-BR-3, AU-565, and EFM-192A cell lines were compared for their degree of signaling nodes phosphorylation at baseline and after trastuzumab-treatment conditions. Representative images of WB assays are depicted, with annotation of the intensity values as obtained by densitometric

Trastuzumab-resistant HER2+ breast cancer cell lines

analysis of the bands (the intensity values of the phosphorylated proteins were normalized to their corresponding total protein bands; non-phosphorylated bands were normalized to GAPDH). Initial seeding was carried out in the absence of treatment, and subsequently trastuzumab was added in a time-dependent manner. Trastuzumab induced changes in phosphorylation dependent on the exposure time. For all experiments, 1.5×10^6 cells/plate were seeded (except for BT-474, in which 1.7×10^6 cells/plate were cultured). Trastuzumab was added at 15 $\mu\text{g}/\text{ml}$ after 24 h of culture and maintained for either 48 h or 72 h more, when cells were then collected for protein extraction. All conditions were therefore processed simultaneously.

gets showing a signal above the median in each cell line 6.82 (0.01-99.23) in BT-474; 5.28 (0.00-133.99) in SK-BR-3; 6.22 (0.00-111.07) in AU-565; and 4.06 (0.01-120.49) in EFM-192A). In particular, the highest signals were measured in the phosphorylation levels of HER2, AKT-Thr308, AKT-Ser473, ERK1/2, and S6RP (**Figure 3B**). Differences between sensitive and resistant cells were observed in AKT-Ser473 (in BT-474), S6RP (in AU-565), and HER2 (both in SK-BR-3 and EFM-192A) ([Supplementary Table 3](#)). In addition, after treatment with trastuzumab, changes occurred in the phosphorylation levels of HER2, AKT-Thr308, AKT-Ser473, ERK1/2, and S6RP. Furthermore, differences in phosphoprotein strength signal between sensitive and resistant cells were observed in AKT-Thr308, AKT-Ser473, ERK1/2, and S6RP in BT474 and AU565, in response to treatment with trastuzumab (**Figure 4**).

Identification of mechanisms of trastuzumab acquired resistance

WB analysis confirmed changes between the parental sensitive and their respective trastuzumab-resistant cell lines (BT-474, BT-474.R, SK-BR-3, SK-BR-3.R, AU-565, AU-565.R, EFM-192A, and EFM-192A.R) that appeared as a consequence of the process of prolonged exposure to trastuzumab (**Figure 4**). Some of those variations were common to all the cell lines, whereas other changes were cell-specific. In general, trastuzumab-resistant populations exhibited higher amounts of HER2 as compared with their respective sensitive cell lines. This matched with an increase in the amounts of pAKT and pERK in the resistant lines (while AKT and ERK showed similar levels to the parental lines), suggesting a higher level of activation of their PI3K and MAPK pathways. Similarly, WB images showed that in the absence of treatment the resistant populations of BT-474 and SK-BR-3 presented increased levels of S6RP and pS6RP (changes in AU-565 and EFM-192A were subtler). These results

suggest that activation of PI3K and/or MAPK pathways are associated with mechanisms of resistance generation in our cell line models, in concordance with previous reports that have found a correlation between increased activation of the PI3K/AKT pathway and resistance to trastuzumab [25].

In addition, when cells were exposed to modulation at different times with 15 $\mu\text{g}/\text{ml}$ of trastuzumab, we confirmed that it down-regulated HER2 receptors in sensitive cells after 2-3 days of treatment (**Figure 4**), thus coinciding with currently proposed primary mechanisms of action for trastuzumab [6, 38]. Phosphorylation levels of pAKT-Ser473 followed a pattern of gradual decay in sensitive and resistant populations of BT-474 and SK-BR-3 that was proportional to time of treatment exposure. Similar changes were observed in sensitive and resistant AU-565 and EFM-192A lines, but only up to 48 h. Similarly, treatment with trastuzumab caused a decrease in pERK levels at 48 h in all the sensitive and resistant cell lines, but the effect did not increase when the exposure to the drug took place over a longer period time. Finally, pS6RP levels were decreased in all sensitive BCCLs when exposed to trastuzumab; this decrease was less relevant in the resistant populations, and did not intensify with further trastuzumab treatment.

Conclusions

In the present study we have generated new cell lines derived from BCCLs through extended exposure to trastuzumab. We validated the identity of the new populations through a study of their molecular profile (ER, PR, and HER2, amplification of *HER2* expression). By studying cell population after treatment with the drug, we also confirmed that those derived lines were resistant to trastuzumab. At the same time, we determined the rate of resistance using the algorithm published by O'Brien. Furthermore, resistance to trastuzumab in established BT-474.R cells was confirmed *in vivo* in a xeno-

graft model. Heterogeneity in the *HER2* amplification profile was observed in most of the BCCLs, revealing a variable percentage of cells without *HER2* amplification, and a wide range of *HER2* copy numbers in all the lines. Using a phospho-antibody array we analyzed the phosphorylated forms of 28 kinase receptors and 11 effectors from different cellular pathways. This revealed that *HER2*, *AKT*, and *S6RP* presented high activity (as indicated by a high degree of phosphorylation) with specific variations between sensitive and resistant populations, depending on the cell line. In addition, we found that several of those pathway targets showed differential expression in their phosphorylation levels between sensitive and resistant lines. Finally, the biochemical study by WB enabled us to characterize patterns of molecular alterations commonly described in breast cancer. Similar to descriptions appearing in the literature, we found that the mechanisms of resistance to trastuzumab that developed in these BCCLs are possibly linked to kinase activation in the *PI3K/AKT* and *MAPK* pathways. These experimental models of breast cancer lines with acquired resistance to trastuzumab are currently being used in our laboratory to gain further insight into the mechanisms of molecular alterations generated during the process of resistance generation, with the ultimate goal of providing useful clinical information that may be used to improve the options of successful therapeutic intervention.

Acknowledgements

The present work was supported by grants from the Spanish Ministry of Economy and Competitiveness (MINECO) (AES Program, grants PI12/01552 and PI15/00934); the Ministry of Health (Cancer Network); and the Community of Madrid (S2010/BMD-2344 grant). S.Z. and C.C. were supported by grants from a Biobanks initiative (Institute of Health Carlos III, RETICS Biobanks Network, with FEDER funding; Fundacion Jimenez Diaz Biobank, RD12/0036/0021). F.R. is recipient of an ISCIII/FEDER intensification program. P.G.-A. is supported by a Fundaci3n Conchita Rábago de Jiménez Díaz grant.

Disclosure of conflict of interest

None.

Authors' contribution

Conception and design: JMG, FR. Development of methodology: SZ, PGA, EMA, JMG, FR. *In vivo* model: OA, AR. Acquisition of data: SZ, PGA, EMA, CC, PE. Analysis and interpretation of data: SZ, PGA, CC, IC, JMG, FR. Writing, review and/or revision of the manuscript: JMG, FR. Administrative, technical, or material support: SZ, PGA, EMA, CC, IC. Study supervision: JA, AL, JMG, FR.

Address correspondence to: Drs. Juan Madoz-Gúrpide and Federico Rojo, Department of Pathology, IIS-Fundación Jiménez Díaz, UAM, Avda, Reyes Católicos 2, E-28040 Madrid, Spain. Tel: +34-915504800; E-mail: JMadoz@fjd.es (JMG); frojo@fjd.es (FR)

References

- [1] Siegel RL, Miller KD and Jemal A. Cancer statistics, 2016. *CA Cancer J Clin* 2016; 66: 7-30.
- [2] Slamon DJ, Clark GM, Wong SG, Levin WJ, Ullrich A and McGuire WL. Human breast cancer: correlation of relapse and survival with amplification of the *HER-2/neu* oncogene. *Science* 1987; 235: 177-182.
- [3] Banerjee S and Smith IE. Management of small *HER2*-positive breast cancers. *Lancet Oncol* 2010; 11: 1193-1199.
- [4] Cho HS, Mason K, Ramyar KX, Stanley AM, Gabelli SB, Denney DW Jr and Leahy DJ. Structure of the extracellular region of *HER2* alone and in complex with the Herceptin Fab. *Nature* 2003; 421: 756-760.
- [5] Romond EH, Perez EA, Bryant J, Suman VJ, Geyer CE Jr, Davidson NE, Tan-Chiu E, Martino S, Paik S, Kaufman PA, Swain SM, Pisansky TM, Fehrenbacher L, Kutteh LA, Vogel VG, Visscher DW, Yothers G, Jenkins RB, Brown AM, Dakhil SR, Mamounas EP, Lingle WL, Klein PM, Ingle JN and Wolmark N. Trastuzumab plus adjuvant chemotherapy for operable *HER2*-positive breast cancer. *N Engl J Med* 2005; 353: 1673-1684.
- [6] Sliwkowski MX, Lofgren JA, Lewis GD, Hotaling TE, Fendly BM and Fox JA. Nonclinical studies addressing the mechanism of action of trastuzumab (Herceptin). *Semin Oncol* 1999; 26: 60-70.
- [7] Baselga J, Albanell J, Molina MA and Arribas J. Mechanism of action of trastuzumab and scientific update. *Semin Oncol* 2001; 28: 4-11.
- [8] Ghosh R, Narasanna A, Wang SE, Liu S, Chakrabarty A, Balko JM, Gonzalez-Angulo AM, Mills GB, Penuel E, Winslow J, Sperinde J, Dua R, Pidaparathi S, Mukherjee A, Litzel K, Kostler

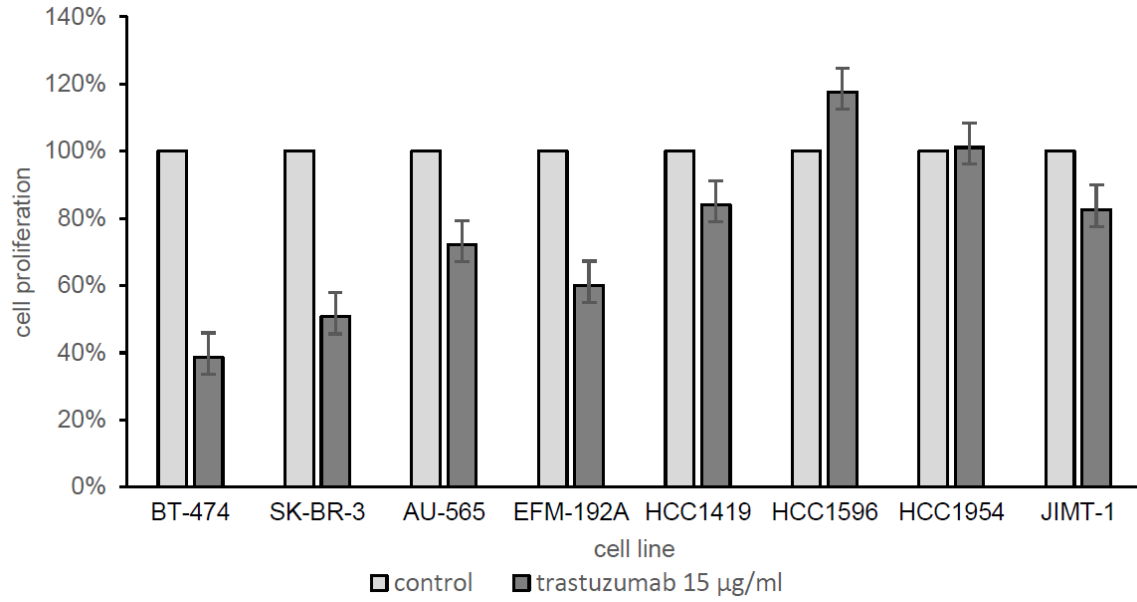
Trastuzumab-resistant HER2+ breast cancer cell lines

- WJ, Lipton A, Bates M and Arteaga CL. Trastuzumab has preferential activity against breast cancers driven by HER2 homodimers. *Cancer Res* 2011; 71: 1871-1882.
- [9] Mayfield S, Vaughn JP and Kute TE. DNA strand breaks and cell cycle perturbation in herceptin treated breast cancer cell lines. *Breast Cancer Res Treat* 2001; 70: 123-129.
- [10] Kauraniemi P, Hautaniemi S, Autio R, Astola J, Monni O, Elkahlon A and Kallioniemi A. Effects of Herceptin treatment on global gene expression patterns in HER2-amplified and nonamplified breast cancer cell lines. *Oncogene* 2004; 23: 1010-1013.
- [11] Motoyama AB, Hynes NE and Lane HA. The efficacy of ErbB receptor-targeted anticancer therapeutics is influenced by the availability of epidermal growth factor-related peptides. *Cancer Res* 2002; 62: 3151-3158.
- [12] Lu YH, Zi XL, Zhao YH, Mascarenhas D and Pollak M. Insulin-like growth factor-I receptor signaling and resistance to trastuzumab (Herceptin). *J Natl Cancer Inst* 2001; 93: 1852-1857.
- [13] Shattuck DL, Miller JK, Carraway KL 3rd and Sweeney C. Met receptor contributes to trastuzumab resistance of Her2-overexpressing breast cancer cells. *Cancer Res* 2008; 68: 1471-1477.
- [14] Agus DB, Akita RW, Fox WD, Lewis GD, Higgins B, Pisacane PI, Lofgren JA, Tindell C, Evans DP, Maiese K, Scher HI and Sliwkowski MX. Targeting ligand-activated ErbB2 signaling inhibits breast and prostate tumor growth. *Cancer Cell* 2002; 2: 127-137.
- [15] Nagata Y, Lan KH, Zhou X, Tan M, Esteva FJ, Sahin AA, Klos KS, Li P, Monia BP, Nguyen NT, Hortobagyi GN, Hung MC and Yu D. PTEN activation contributes to tumor inhibition by trastuzumab, and loss of PTEN predicts trastuzumab resistance in patients. *Cancer Cell* 2004; 6: 117-127.
- [16] Yakes FM, Chinratanalab W, Ritter CA, King W, Seelig S and Arteaga CL. Herceptin-induced inhibition of phosphatidylinositol-3 kinase and Akt is required for antibody-mediated effects on p27, cyclin D1, and antitumor action. *Cancer Res* 2002; 62: 4132-4141.
- [17] Scaltriti M, Eichhorn PJ, Cortes J, Prudkin L, Aura C, Jimenez J, Chandarlapaty S, Serra V, Prat A, Ibrahim YH, Guzman M, Gili M, Rodriguez O, Rodriguez S, Perez J, Green SR, Mai S, Rosen N, Hudis C and Baselga J. Cyclin E amplification/overexpression is a mechanism of trastuzumab resistance in HER2+ breast cancer patients. *Proc Natl Acad Sci U S A* 2011; 108: 3761-3766.
- [18] Le XF, Claret FX, Lammayot A, Tian L, Deshpande D, LaPushin R, Tari AM and Bast RC Jr. The role of cyclin-dependent kinase inhibitor p27Kip1 in anti-HER2 antibody-induced G1 cell cycle arrest and tumor growth inhibition. *J Biol Chem* 2003; 278: 23441-23450.
- [19] Arribas J, Baselga J, Pedersen K and Parra-Palau JL. p95HER2 and breast cancer. *Cancer Res* 2011; 71: 1515-1519.
- [20] Sun Z, Shi Y, Shen Y, Cao L, Zhang W and Guan X. Analysis of different HER-2 mutations in breast cancer progression and drug resistance. *J Cell Mol Med* 2015; 19: 2691-2701.
- [21] Uphoff CC and Drexler HG. Detection of mycoplasma contaminations in cell cultures by PCR analysis. *Hum Cell* 1999; 12: 229-236.
- [22] Bustin SA, Benes V, Garson JA, Hellemans J, Huggett J, Kubista M, Mueller R, Nolan T, Pfaffl MW, Shipley GL, Vandesompele J and Wittwer CT. The MIQE guidelines: minimum information for publication of quantitative real-time PCR experiments. *Clin Chem* 2009; 55: 611-622.
- [23] Uphoff CC, Denkmann SA and Drexler HG. Treatment of mycoplasma contamination in cell cultures with Plasmocin. *J Biomed Biotechnol* 2012; 2012: 267678.
- [24] Zhang S, Huang WC, Li P, Guo H, Poh SB, Brady SW, Xiong Y, Tseng LM, Li SH, Ding Z, Sahin AA, Esteva FJ, Hortobagyi GN and Yu D. Combating trastuzumab resistance by targeting SRC, a common node downstream of multiple resistance pathways. *Nat Med* 2011; 17: 461-469.
- [25] O'Brien NA, Browne BC, Chow L, Wang Y, Ginther C, Arboleda J, Duffy MJ, Crown J, O'Donovan N and Slamon DJ. Activated phosphoinositide 3-kinase/AKT signaling confers resistance to trastuzumab but not lapatinib. *Mol Cancer Ther* 2010; 9: 1489-1502.
- [26] McDermott M, Eustace AJ, Busschots S, Breen L, Crown J, Clynes M, O'Donovan N and Stordal B. In vitro Development of Chemotherapy and Targeted Therapy Drug-Resistant Cancer Cell Lines: A Practical Guide with Case Studies. *Front Oncol* 2014; 4: 40.
- [27] Wolff AC, Hammond MEH, Hicks DG, Dowsett M, McShane LM, Allison KH, Allred DC, Bartlett JMS, Bilous M, Fitzgibbons P, Hanna W, Jenkins RB, Mangu PB, Paik S, Perez EA, Press MF, Spears PA, Vance GH, Viale G and Hayes DF. Recommendations for Human Epidermal Growth Factor Receptor 2 Testing in Breast Cancer: American Society of Clinical Oncology/ College of American Pathologists Clinical Practice Guideline Update. *Arch Pathol Lab Med* 2013; 138: 241-256.
- [28] Wolff AC, Hammond ME, Hicks DG, Dowsett M, McShane LM, Allison KH, Allred DC, Bartlett JM, Bilous M, Fitzgibbons P, Hanna W, Jenkins RB, Mangu PB, Paik S, Perez EA, Press MF, Spears PA, Vance GH, Viale G, Hayes DF; American Society of Clinical Oncology; College

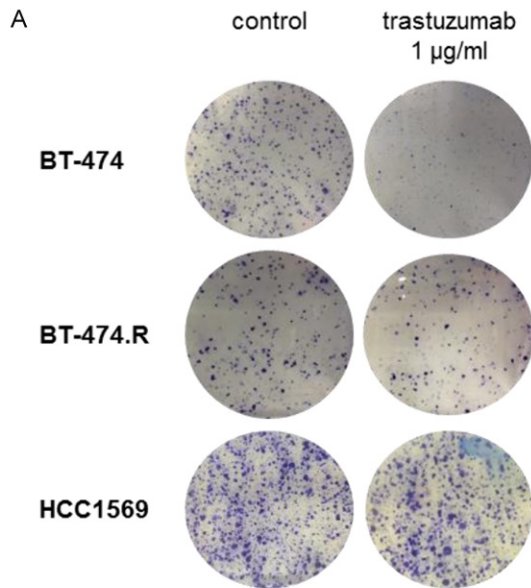
Trastuzumab-resistant HER2+ breast cancer cell lines

- of American Pathologists. Recommendations for human epidermal growth factor receptor 2 testing in breast cancer: American Society of Clinical Oncology/College of American Pathologists clinical practice guideline update. *J Clin Oncol* 2013; 31: 3997-4013.
- [29] Meacham CE and Morrison SJ. Tumour heterogeneity and cancer cell plasticity. *Nature* 2013; 501: 328-337.
- [30] Burrell RA, McGranahan N, Bartek J and Swanton C. The causes and consequences of genetic heterogeneity in cancer evolution. *Nature* 2013; 501: 338-345.
- [31] Nowell PC. The clonal evolution of tumor cell populations. *Science* 1976; 194: 23-28.
- [32] Gijzen M, King P, Perera T, Parker PJ, Harris AL, Larijani B and Kong A. HER2 phosphorylation is maintained by a PKB negative feedback loop in response to anti-HER2 herceptin in breast cancer. *PLoS Biol* 2010; 8: e1000563.
- [33] Junttila TT, Akita RW, Parsons K, Fields C, Phillips GDL, Friedman LS, Sampath D and Sliwkowski MX. Ligand-Independent HER2/HER3/PI3K Complex Is Disrupted by Trastuzumab and Is Effectively Inhibited by the PI3K Inhibitor GDC-0941. *Cancer Cell* 2009; 15: 429-440.
- [34] Gennari R, Menard S, Fagnoni F, Ponchio L, Scelsi M, Tagliabue E, Castiglioni F, Villani L, Magalotti C, Gibelli N, Oliviero B, Ballardini B, Da Prada G, Zambelli A and Costa A. Pilot study of the mechanism of action of preoperative trastuzumab in patients with primary operable breast tumors overexpressing HER2. *Clin Cancer Res* 2004; 10: 5650-5655.
- [35] Arnould L, Gelly M, Penault-Llorca F, Benoit L, Bonnetain F, Migeon C, Cabaret V, Fermeaux V, Bertheau P, Garnier J, Jeannin JF and Coudert B. Trastuzumab-based treatment of HER2-positive breast cancer: an antibody-dependent cellular cytotoxicity mechanism? *Br J Cancer* 2006; 94: 259-267.
- [36] Nahta R and Esteva FJ. HER2 therapy: molecular mechanisms of trastuzumab resistance. *Breast Cancer Res* 2006; 8: 215.
- [37] Diermeier S, Horvath G, Knuechel-Clarke R, Hofstaedter F, Szollosi J and Brockhoff G. Epidermal growth factor receptor coexpression modulates susceptibility to Herceptin in HER2/neu overexpressing breast cancer cells via specific erbB-receptor interaction and activation. *Exp Cell Res* 2005; 304: 604-619.
- [38] Cuello M, Ettenberg SA, Clark AS, Keane MM, Posner RH, Nau MM, Dennis PA and Lipkowitz S. Down-regulation of the erbB-2 receptor by trastuzumab (herceptin) enhances tumor necrosis factor-related apoptosis-inducing ligand-mediated apoptosis in breast and ovarian cancer cell lines that overexpress erbB-2. *Cancer Res* 2001; 61: 4892-4900.

Trastuzumab-resistant HER2+ breast cancer cell lines



Supplementary Figure 1. Assessment of sensitivity to trastuzumab in eight HER2-positive BCCLs. The sensitivity to trastuzumab was assessed by testing cell proliferation in the presence and absence of 15 µg/ml trastuzumab for 7 days. Control cell lines grown in the absence of drug were represented as light gray columns; proliferation of treated cells is shown in dark gray columns.

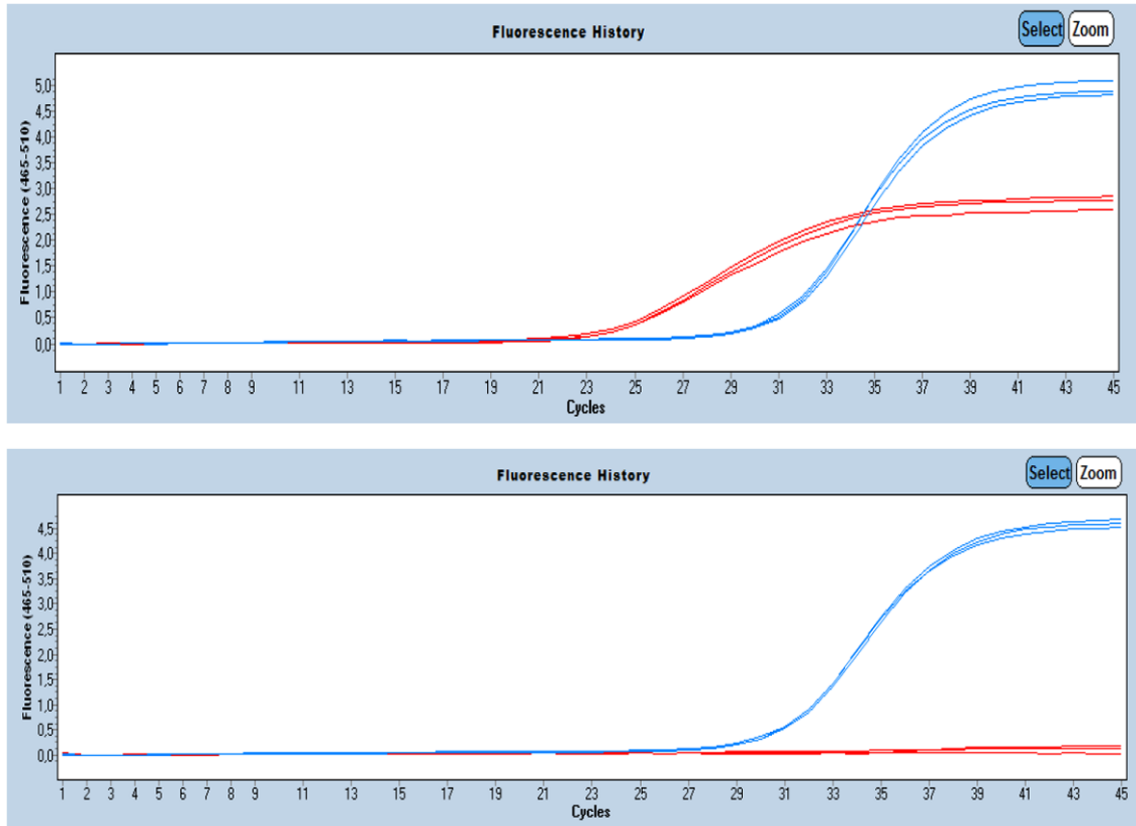


Supplementary Figure 2. A. Cells treated for prolonged periods of time with trastuzumab were more resistant to further exposure to the drug, as seen in a clonogenic assay. B. BT-474.R cells improved their proliferation rates with respect to the parental BT-474 line after 21 days of trastuzumab treatment, close to the competence of the primary-resistance HCC1569 cell line. They improved the number of colonies, their size, and the area of coverage.

B

cell line	count		average size		% area	
	control	trastuzumab 1 µg/ml	control	trastuzumab 1 µg/ml	control	trastuzumab 1 µg/ml
BT-474	100%	61%	73.07	28.44	100%	24%
BT-474.R	100%	78%	111.81	91.35	100%	63%
HCC1569	100%	103%	137.30	121.87	100%	99%

Trastuzumab-resistant HER2+ breast cancer cell lines



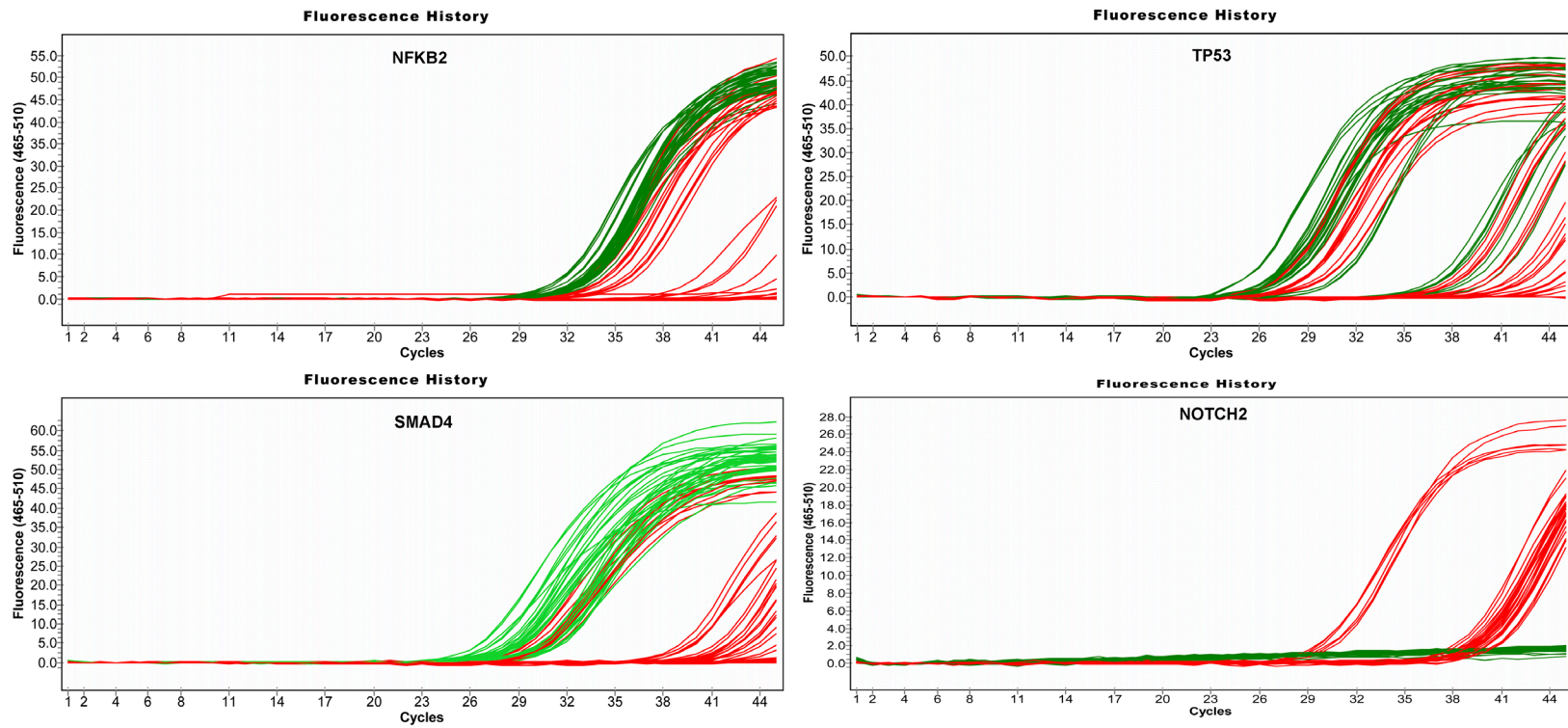
Supplementary Figure 3. Detection of *Mycoplasma* contamination in BCCL by home-made qPCR assays. Amplification curves in red in the first panel indicate the presence of bacteria of the genus *Mycoplasma spp.* The red flat lines in the second panel illustrate the absence of bacterial contamination. Curves in blue show the amplification signal for *RPP30* (RNaseP).

Supplementary Table 1. Detection of *Mycoplasma* contamination in BCCL by home-made qPCR assays

Cell lines	Mycoplasma assay	
	Cp average	Cp deviation
BT-474	25.84	0.00
BT-474.R	40.00	0.00
SK-BR-3	20.76	0.65
SK-BR-3.R	33.79	0.00
AU-565	40.00	0.00
AU-565.R	34.18	0.00
EFM-192A	23.45	0.05
EFM-192A.R	22.34	0.07

Average values of amplification cycles lower than 30 are symptomatic of contamination; values greater than 30 indicate absence of infection.

Trastuzumab-resistant HER2+ breast cancer cell lines



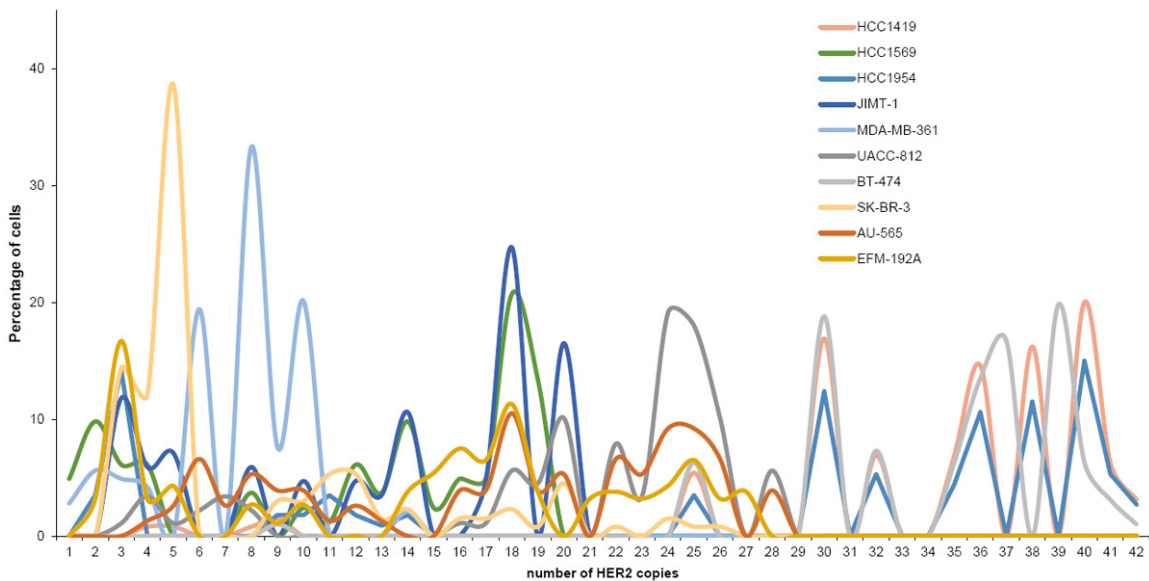
Supplementary Figure 4. The molecular mutational profiling of the BCCL included in the study confirmed their identity. The plots show the qPCR amplification curves obtained for the detection of mutations in specific identification genes. The curves indicate the cycle at which each sample is amplified, so curves with earlier C_p indicate that amplification has occurred.

Trastuzumab-resistant HER2+ breast cancer cell lines

Supplementary Table 2. Differential of Cp for the amplification curves between the wt and mutant assays for every BCCL

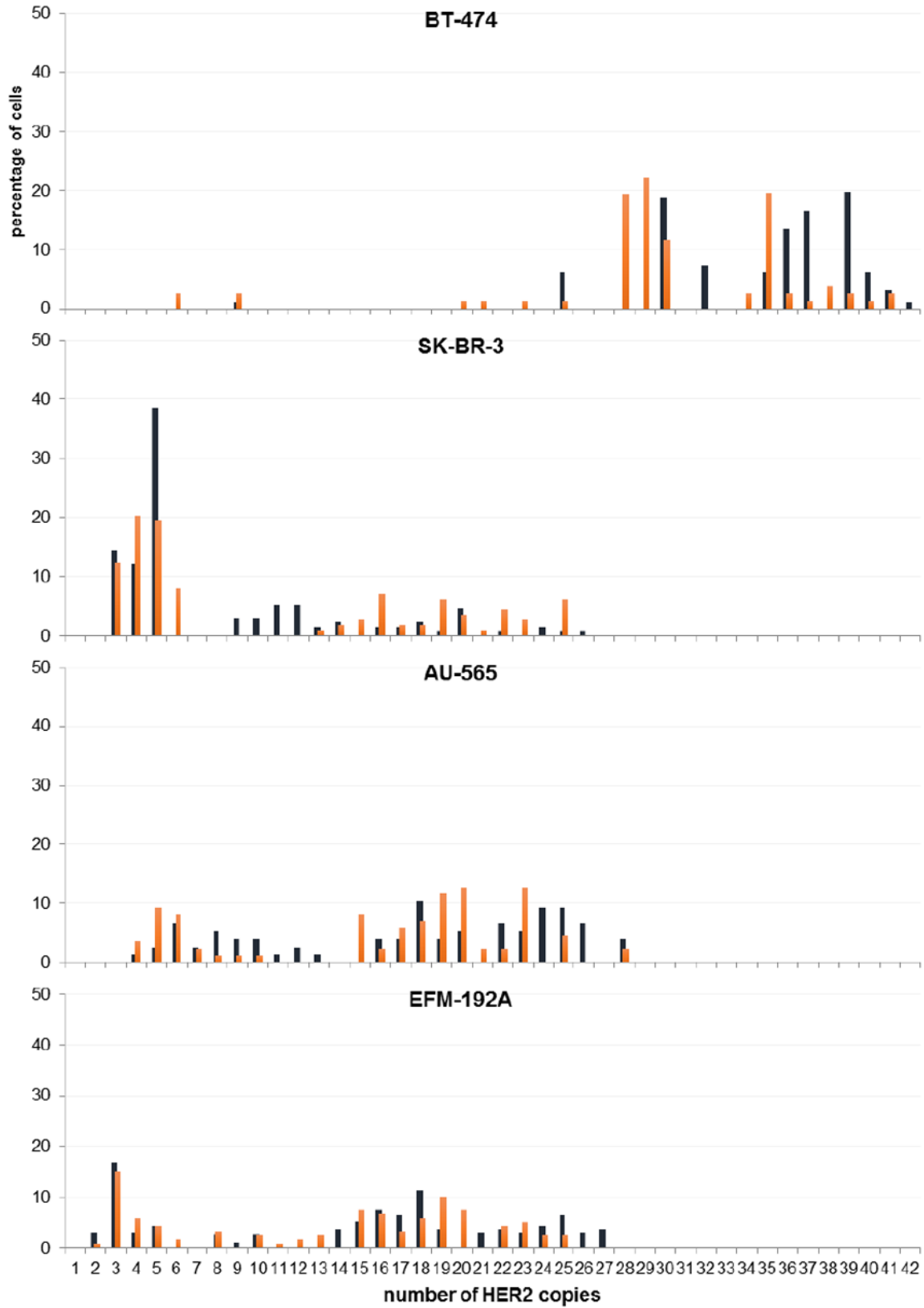
BCCL	Mutation											
	NFKB2			TP53			SMAD4			NOTCH2		
	wt	mut	Δ	wt	mut	Δ	wt	mut	Δ	wt	mut	Δ
BT-474	30.87	31.86	0.99	26.59	37.61	11.02	28.52	40.00	11.47	45.00	45.00	0.00
BT-474.R	30.87	31.96	1.09	26.87	38.76	11.89	28.03	40.00	11.97	45.00	45.00	0.00
SK-BR-3	31.34	40.00	8.66	35.10	28.24	-6.87	33.64	45.00	11.36	45.00	45.00	0.00
SK-BR-3.R	31.93	38.22	6.30	35.11	28.65	-6.46	30.91	40.00	9.09	45.00	45.00	0.00
AU-565	31.28	39.44	8.16	35.47	28.07	-7.40	33.77	35.25	1.48	45.00	45.00	0.00
AU-565.R	32.16	40.00	7.84	37.10	29.06	-8.05	34.84	36.22	1.38	45.00	45.00	0.00
EFM-192A	31.29	38.29	7.00	27.65	39.38	11.73	33.62	45.00	11.38	45.00	29.88	-15.12
EFM-192A.R	31.71	40.00	8.30	28.23	39.31	11.09	36.17	45.00	8.83	45.00	30.87	-14.13

The values highlighted in bold are indicative of the presence of mutation for those given genes and cell lines.



Supplementary Figure 5. Genetic heterogeneity among cancer cell lines populations was exposed in our study as *HER2* copy number was investigated in 10 BCCLs. FISH analyses detected *HER2* amplification based on *HER2*/CEP17 (red/green signal signals) ratio. 60 cell nuclei were counted per sample. All the cell lines presented a wide range of *HER2* copy number, with different percentages of cells between lines carrying low and high amplification numbers.

Trastuzumab-resistant HER2+ breast cancer cell lines



Supplementary Figure 6. Sensitive BCCLs and their corresponding derived-resistant populations showed a comparable pattern of *HER2* copy number. FISH analyses confirmed a similar profile of percentage of cells against number of copies for every pair of parental/resistant cell line, as depicted here. This variation is illustrative of the

Trastuzumab-resistant HER2+ breast cancer cell lines

heterogeneity of tumor cell populations. At the same time this matching between pairs of parental/resistant cell lines confirmed the identity of the resistant-derived lines. Parental, sensitive cell lines are depicted in black-colored columns; resistant cells in orange.

Supplementary Table 3. Several tyrosine kinases involved in signaling nodes were differentially regulated following the generation of resistance to trastuzumab in BCCL

Target	Cell line			
	BT-474	SK-BR-3	AU-565	EFM-192A
HER2	-0.1	1.3	-0.2	-1.3
AKT(Thr308)	0.8	-1.0	0.2	-2.2
AKT(Ser473)	1.4	-0.4	0.2	-0.8
ERK1/2	-0.3	-0.4	0.2	0.5
S6RP	-0.3	-0.1	1.3	-0.1

Phosphorylation levels for 28 receptors and 11 effectors were measured by incubation of protein extracts from BT-474, SK-BR-3, AU-565, and EFM-192A cell lines (both sensitive and resistant lines) in antibody arrays for phosphorylated species. Signal intensities were normalized to the positive control in the array, FC were calculated for relative signal between resistant vs. sensitive cell lines, and finally data were calculated as $\text{Log}_2[\text{FC}(\text{R}/\text{S})]$.